# Temporal Distribution Patterns of Cryptic Brachionus calyciflorus (Rotifera) Species in Relation to Biogeographical Gradient Associated with Latitude

Yuan Xu , Le-Le Ge , Xin-Feng Cheng , Xian-Ling Xiang , Xin-Li Wen , Yong-Jin Wang , Hao Fu , Ya-Li Ge * , Yi-Long Xi *

Posted Date: 14 December 2023

doi: 10.20944/preprints202312.1103.v1

Keywords: cryptic species; seasonal succession; temporal overlap; environmental variables; climatic zone

*Article*

# Temporal Distribution Patterns of Cryptic *Brachionus calyciflorus* (Rotifera) Species in Relation to Biogeographical Gradient Associated with Latitude

**Yuan Xu [1,2], Le-Le Ge [1,2], Xin-Feng Cheng [1,2], Xian-Ling Xiang [1,2], Xin-Li Wen [1,2], Yong-Jin Wang [3], Hao Fu [4], Ya-Li Ge [1,2,*] and Yi-Long Xi [1,2,*]**

[1] School of Ecology and Environment, Anhui Normal University, Wuhu 241002, Anhui Province, China
[2] Collaborative Innovation Center of Recovery and Reconstruction of Degraded Ecosystem in Wanjiang Basin Co-funded by Anhui Province and Ministry of Education of the People's Republic of China, Anhui Normal University, Wuhu 241002, Anhui Province, China
[3] Management Committee of Scenic Attraction of Lake Yunlong, Xuzhou 221007, Jiangsu Province, China
[4] Reservoir Management Office of Lake Yunlong, Xuzhou 221007, Jiangsu Province, China
* Correspondence: geyali98@163.com (Y.L.G.); ylxi1965@126.com (Y.L.X)

**Simple Summary:** In subtropical shallow lakes, large-scale changes in water temperature lead to seasonal succession of some cryptic rotifer species, and temporal overlap of other cryptic rotifer species is a common phenomenon. In tropical shallow lakes, however, relatively stable water temperature throughout the year may not lead to seasonal succession of cryptic rotifer species, but evidence is scarce. Studies on the temporal distribution patterns of cryptic *Brachionus calyciflorus* species in three lakes in China revealed that in the warm-temperate Lake Yunlong, *B. fernandoi* and *B. calyciflorus* s.s. underwent a seasonal succession, which was largely attributed to their differential adaptation to water temperature. In the subtropical Lake Jinghu, *B. fernandoi*, *B. calyciflorus* s.s. and *B. dorcas* exhibited both seasonal succession and temporal overlap. Seasonal successions were largely attributed to their differential adaptation to temperature, and temporal overlap resulted from their differential responses to algal food concentration. In the tropical Lake Jinniu, *B. calyciflorus* s.s. persisted throughout the year, and overlapped with *B. dorcas* for 5 months. Temporal overlap resulted from their differential responses to copepod predation. These results indicated that the temporal distribution pattern of cryptic *B. calyciforus* species and the mechanism allowing competitor coexistence vary with different climate zones.

**Abstract:** Sympatric distribution and temporal overlap of cryptic zooplankton species pose a challenge to the framework of the niche differentiation theory and the mechanisms allowing competitor coexistence. We applied the methods of phylogenetic analysis, DNA taxonomy and statistical analysis to study the temporal distribution patterns of cryptic *B. calyciflorus* species, an excellent model, in three lakes, and to explore the putative mechanisms for their seasonal succession and temporal overlap. The results showed that in the warm-temperate Lake Yunlong, *B. fernandoi* and *B. calyciflorus* s.s. underwent a seasonal succession, which was largely attributed to their differential adaptation to water temperature. In the subtropical Lake Jinghu, *B. fernandoi*, *B. calyciflorus* s.s. and *B. dorcas* exhibited both seasonal succession and temporal overlap. Seasonal successions were largely attributed to their differential adaptation to temperature, and temporal overlap resulted from their differential responses to algal food concentration. In the tropical Lake Jinniu, *B. calyciflorus* s.s. persisted throughout the year, and overlapped with *B. dorcas* for 5 months. Temporal overlap resulted from their differential responses to copepod predation. These results indicated that the temporal distribution pattern of cryptic *B. calyciforus* species and the mechanism allowing competitor coexistence vary with different climate zones.

**Keywords:** rotifers; cryptic species; seasonal succession; temporal overlap; environmental variables; climatic zone

 doi:10.20944/preprints202312.1103.v1



## 1. Introduction

In recent two decades, the use of DNA taxonomy and also integrative approaches combining morphological, ecological and molecular data has revealed the existence of cryptic species in a broad range of taxonomic groups [1–5]. As species belonging to the same cryptic species complex are so similar in their morphology and physiology, a high degree of ecological similarity and hence competitive exclusion is expected to occur between them [6,7]. However, cryptic species commonly exist in sympatry [6,8–10], which poses a challenge to the framework of the niche differentiation theory and the mechanisms allowing competitor coexistence [7,11–13].

Phylum Rotifera is one of the groups of animals with the highest level of occurrence of cryptic species complexes. Up to now, 54 cryptic rotifer species complexes have been discovered [13]. Among them, the euryhaline *Brachionus plicatilis* species complex has been the subject of many studies on the temporal distribution patterns of cryptic rotifer species and the mechanisms allowing competitor coexistence. Previous studies have shown that the temporal distribution of cryptic *B. plicatilis* species generally displays both seasonal succession and temporal overlap [8,14–18]. Seasonal succession is largely attributed to their differential adaptation to salinity and/or temperature [8,14–21], and temporal overlap results from their differential responses to environmental conditions such as salinity [8,14–16,20,21] and oxygen availability [22], resource partitioning and differential vulnerability to predators [23–25].

The freshwater *B. calyciflorus* species complex has also received attention in studies n the temporal distribution patterns of cryptic rotifer species and the mechanisms allowing competitor coexistence. The studies on this species complex inhabiting a warm-temperate pond and several subtropical shallow lakes have revealed that temporal distribution of cryptic *B. calyciflorus* species generally displays both seasonal succession and temporal overlap [26–30]. Seasonal succession of *B. fernandoi*, and *B. calyciforus* s.s. and *B. dorcas* is largely attributed to their differential adaptation to temperature [30–32] and temporal overlap of *B. calyciforus* s.s. and *B. dorcas* results from their differential responses to algal food concentration [26,29,30].

The warm-temperate ponds and subtropical shallow lakes inhabited by the *B. calyciflorus* complex have low spatial heterogeneity but high temporal variability, of which the most obvious is the seasonal variation of water temperature [26–30]. In tropical shallow lakes, however, relatively stable water temperature throughout the year may not lead to seasonal succession of cryptic *B. calyciflorus* species, but evidence is scarce. To further explore the role of temperature in shaping the occurrence and distribution of the species within the *B. calyciforus* complex, it would be worthwhile to investigate the possibility of a biogeographical gradient associated with latitude, which could be connected to variations in water temperature [13].

In this study, we applied the methods of phylogenetic analysis, DNA taxonomy and principal component analysis to investigate the temporal distribution patterns of cryptic *B. calyciflorus* species in three lakes in China: the warm-temperate Lake Yunlong, subtropical Lake Jinghu and tropical Lake Jinniu, and to explore the putative mechanisms for their seasonal succession and/or temporal overlap. We tested the following hypotheses: i) the temporal distribution pattern of cryptic *B. calyciforus* species varies with different climate zones; and ii) the mechanisms underlying the temporal overlap of potentially strong competitors are different between climate zones.

## 2. Materials and Methods

### *2.1. Sample collection and environment variables analyses*

Zooplankton samplings were monthly carried out in Yunlong, Jinghu and Jinniu lakes from October 2018 to September 2019. Lake Yunlong (34.24°N, 117.17°E) is located in Xuzhou city, Jiangsu Province, and has a surface area of 6.76 km$^2$ with an average water depth of 2.5 m. Lake Jinghu (31.33°N, 118.37°E) is located in Wuhu city, Anhui Province, and has a surface area of 0.15 km$^2$ with an average water depth of 1.5 m. Lake Jinniu (20.01°N, 110.32°E) is located in Haikou city, Hainan Province, and has a surface area of 1.98 km$^2$ with an average water depth of 2.0 m. On each occasion, two quantitative zooplankton samples were obtained from two fixed sites of each lake by filtering

 doi:10.20944/preprints202312.1103.v1



(25 μm mesh net) two samples of integrated lake water (5 L of water from the surface to the bottom at 0.5 m intervals) and fixing *in situ* with 4% formaldehyde. From these quantitative samples, the density estimates of the *B. calyciflorus* species complex and its potential competitors and predators, including cladocerans, omnivorous rotifers (e.g. *Asplanchna* spp.) and copepods, were calculated by direct counts of females under an Olympus BH-2 microscope with 100 × magnifications. Additional two zooplankton samples were also collected at the fixed sites of each lake in several hauls using a 25-μm plankton net, fixing *in situ* with 90% ethanol, and then transported to the laboratory. Under a stereo-microscope, individuals belonging to the *B. calyciflorus* species complex were isolated from each sample, washed several times with double distilled water, and preserved at -20°C until molecular processing.

Simultaneously with the collection of zooplankton samples, water temperature, pH value, and dissolved oxygen (DO), total nitrogen (TN), total phosphorus (TP) and ammonium-nitrogen ($NH_4^+$-N) concentrations were measured, as described in details by [33]. The chlorophyll *a* (Chl-*a*) concentration of the other integrated water sample filtered through a 25-μm mesh net were also measured as a proxy for the availability of relatively small phytoplankton that might be a food resource for rotifers, according to Huang [34].

### *2.2. DNA extraction, PCR amplification and sequencing*

The HotSHOT technique [35] was used to extract DNA from individual rotifers. An individual rotifer was transferred into a 0.2 ml EP tube containing 30 μl of alkaline lysis buffer under a stereomicroscope. Once in the buffer, the rotifer was crushed against the side of the tube using a sterile pipette tip. The sample was incubated at 95 °C for 30 min and stored on ice for 3-4 min. After a further 30 μl of neutralizing buffer was added to the EP tube, the sample was vortexed briefly and spun down, and then stored at -20 °C.

PCR amplification was conducted using the iCycler PCR machine (Bio-Rad Research Company). The primers for the mitochondrial cytochrome c oxidase subunit I (mtCOI) gene sequence were HCO2198 (5'-TAAACTTCAGGGTGACCAAAAAATCA-3') and LCO1490 (5'-GGTCAACAAATCA TAAAGATATTGG-3') [36], and those for the nuclear internal transcribed spacer 1 locus (nuITS1) sequence were LH2 (5′-GTCGAATTCGTAGGTGAACCTGCGGAAGGATCA-3′) and Dlam (5′-CCTGCAGTCGACAKATGCTTAARTTCAGCRGG-3′) [37]. All reagents and primers were obtained from Sangon Biotechnology Co. Ltd (Shanghai, China). A 25-μl amplification system for mtCOI sequences consisted of 2.5 μl of 10 × PCR buffer, 0.5 μl of each primer (0.01 mM), 2 μl of $MgCl_2$ (25 mM), 2 μl of each dNTP (25 mM), 5.0 μl of template DNA, and 0.4 μl of *Taq* DNA polymerase (Takara). Amplification of the mtCOI sequence was performed using the following cycling conditions: pre-denaturation at 95 °C for 5 min and 35 cycles of denaturation at 94 °C for 40 s, annealing at 48 °C for 30 s, elongation at 72 °C for 2 min and final extension at 72 °C for 20 min. A 25-μl amplification system for nuITS1 sequences consisted of 2.5 μl of 10 × PCR buffer, 0.5 μl of each primer (0.01 mM), 2 μl of $MgCl_2$ (25 mM), 2 μl of each dNTP (25 mM), 5.0 μl of template DNA, and 0.5 μl of *Taq* DNA polymerase (Takara). Amplification of the nuITS1 sequence was performed using the following cycling conditions: pre-denaturation at 95 °C for 5 min and 35 cycles of denaturation at 94 °C for 30 s, annealing at 48 °C for 30 s, elongation at 72 °C for 1 min and final extension at 72 °C for 10 min. After electrophoresis on 0.8% agarose gels, the PCR products were sequenced using an ABI-PRISM 3730 automated sequencer.

### *2.3. Sequence alignment and phylogenetic analyses*

All sequences were aligned individually using the default settings of the online version (http://blast.ncbi.nlm.nih.gov/Blast.cgi) of BLAST [38]. Fragments of 632 bp and 270 bp were selected as the mtCOI and nuITS1 target sequences, respectively.

The phylogenetic relationships were reconstructed using two optimality criteria: Maximum Likelihood (ML) and Bayesian Inference (BI). The most optimal sequence evolution parameters and models (TVMþG and GTRþG), as selected by Modeltest 3.7 [39], were used as settings in PAUP and Bayesian phylogenetic analyses based on the mtCOI and nuITS1 sequences. Two independent

 doi:10.20944/preprints202312.1103.v1



Bayesian analyses with the Markov Chain Monte Carlo (MCMC) method were conducted in MrBayes 3.1.2 [40], with four chains per analysis and randomly chosen starting trees. The Markov chains were run for 10,000,000 generations with trees being sampled every 100 generations. The first 250,000 generations were discarded as burn-in, and the remaining trees were used to estimate Bayesian posterior probabilities. In order to discriminate the lineage relationships between COI/ITS1 groups within the *B. calyciflorus* species complex found in this study, and demonstrated by Xiang et al. [41,42] and Papakostas et al. [43], five mtCOI and nuITS1 sequences of *B. calyciflorus* species complex were obtained from GenBank (the accession number of the five mtCOI sequences are AQ_W13_GU232548, DZ_W2_GU232575, TJ_S10_FJ826940, WH_S23_FJ826934 and XZ_W2_GU232725; accordingly, those of the five nuITS1 squences are AQ_W13_FJ937455, DZ_W2_FJ937482, TJ_S10_GU012757, WH_S23_GU012785 and XZ_W2_FJ937632) and used for phylogenetic analysis. The sequences of a cryptic *B. plicatilis* species (GenBank accession number of the mtCOI and nuITS1 sequences are JX293046 and KU299746) were used as outgroup in the phylogenetic reconstruction based on the mtCOI and nuITS1 sequences, respectively.

### *2.4. COI/ITS1 group diagnosis and abundance estimation*

Three main types of species-delimitation methods, including the Automatic Barcode Gap Discovery (ABGD), Poisson Tree Process (PTP), and Generalized Mixed Yule Coalescent (GMYC) models [44,45], were applied to explore the number of reproductively isolated COI/ITS1 groups in the *B. calyciflorus* species complex. The ABGD model (available from http://wwwabi.snv.jussieu.fr/public/abgd/abgdweb.html) was applied to automatically discover the barcode gap instead of using one or several predefined distance thresholds for COI/ITS1 group delimitation [46]. The PTP model was applied to the input ML trees using coalescence theory to distinguish species/group [47]. The PTP method was used through the online tool (http://species.h-its.org/) with default settings, and the output of the ML and BI optimization algorithms was reported. An ultrametric tree was constructed based on Bayesian analysis using the penalized likelihood (PL) method and the truncated Newton (TN) algorithm on r8s software [48], and then a GMYC model with multiple thresholds was run on the ultrametric gene tree with R software [49,50] to identify potential COI/ITS1 group representing independently evolving entities. In the case of discordance in the amount of splitting, we chose to keep the smallest number of entities to avoid over-splitting the species complex [45].

Because different COI/ITS1 groups in the *B. calyciflorus* species complex are difficult to be visually discriminated under a microscope [51], the density of each COI/ITS1 group in the *B. calyciflorus* species complex at each sampling date in each lake was calculated as $d_i = d_c \times p_i$, where $d_i$, $d_c$, and $p_i$ indicates the density of the $i^{th}$ COI/ITS1 group, the density of the species complex, and the relative frequency of $i^{th}$ COI/ITS1 group, respectively. The relative frequency of each COI/ITS1 group ($p_i$) was derived from the DNA data analysis and was calculated with $p_i = n_i/n$, where $n_i$ and $n$ represents the individual numbers of the $i^{th}$ COI/ITS1 group and the individual numbers of the species complex, respectively [8,16,30].

### *2.5. Data analysis*

In order to investigate the most influential variables among environmental variables (temperature, pH, DO, chl-*a* concentration, and the densities of *Asplanchna*, copepods and cladocerans) in each of the three lakes, a principal component analysis (PCA) was carried out based on the covariance matrix of these variables using the program PAST [31]. Three variables (the densities of *Asplanchna*, copepods and cladocerans) in both Lake Yunlong and Lake Jinghu, and five variables (water temperature, TP and dissolved oxygen concentrations, and the densities of *Asplanchna* and cladocerans) in Lake Jinniu were very strongly skewed and were transformed to lg ($x$+1) or lg $x$ (only for water temperature) [32]. After the PCA analysis, the frequency pie chart of COI/ITS1 group in the *B. calyciflorus* species complex for each sampling was placed at the respective sampling position on the two-dimensional space. Thus, the relationship was determined between the COI/ITS1 group frequency and each environmental variable [8,30]. Subsequently, the effects of the most influential

 doi:10.20944/preprints202312.1103.v1



variables on the relative frequency and density of each COI/ITS1 group were measured by a generalized linear model (GLM) analysis of deviance with a Poisson distribution and a logit link function in R2.13.0 [52].

**Table 1.** Summary information for each sample.

| Sample code | Collection date | Sample size | Tem (°C) | pH | Chl-*a* (μg l$^{-1}$) | DO (mg l$^{-1}$) | TN (mg l$^{-1}$) | TP (mg l$^{-1}$) | $NH_4^+$-N (mg l$^{-1}$) |
|---|---|---|---|---|---|---|---|---|---|
| **Lake Yunlong** | | | | | | | | | |
| YL10 | Oct 2018 | 23 | 16.7 | 7.73 | 25.12 | 8.90 | 1.29 | 0.133 | 0.31 |
| YL11 | Nov 2018 | 7 | 10.9 | 8.16 | 22.39 | 1.42 | 1.61 | 0.090 | 0.33 |
| YL12 | Dec 2018 | 40 | 4.9 | 8.2 | 13.65 | 3.90 | 1.48 | 0.067 | 0.32 |
| YL01 | Jan 2019 | 19 | 3.7 | 8.85 | 8.19 | 2.14 | 2.32 | 0.046 | 0.41 |
| YL02 | Feb 2019 | 19 | 3.2 | 8.77 | 5.46 | 2.30 | 1.96 | 0.057 | 0.34 |
| YL03 | Mar 2019 | 15 | 14.0 | 8.6 | 26.75 | 1.97 | 1.96 | 0.058 | 0.46 |
| YL04 | Apr 2019 | 16 | 18.9 | 6.94 | 36.04 | 1.35 | 2.27 | 0.062 | 0.21 |
| YL05 | May 2019 | 30 | 23.6 | 8.92 | 33.85 | 1.74 | 1.91 | 0.065 | 0.33 |
| YL06 | Jun 2019 | 33 | 28.7 | 9.06 | 27.30 | 1.94 | 1.99 | 0.073 | 0.36 |
| YL07 | Jul 2019 | 26 | 28.3 | 8.92 | 66.07 | 1.13 | 1.37 | 0.092 | 0.40 |
| YL08 | Aug 2019 | 42 | 28.6 | 9.22 | 60.61 | 1.52 | 2.02 | 0.069 | 0.41 |
| YL09 | Sep 2019 | 20 | 23.0 | 8.48 | 50.23 | 1.53 | 1.90 | 0.095 | 0.44 |
| Lake Jinghu | | | | | | | | | |
| JH10 | Oct 2018 | 18 | 19.5 | 8.72 | 20.75 | 1.38 | 0.96 | 0.087 | 0.04 |
| JH11 | Nov 2018 | 17 | 5.6 | 8.93 | 19.66 | 2.66 | 0.93 | 0.073 | 0.04 |
| JH12 | Dec 2018 | 16 | 5.6 | 7.90 | 15.29 | 2.30 | 1.11 | 0.048 | 0.04 |
| JH01 | Jan 2019 | 20 | 8.0 | 9.16 | 10.37 | 2.35 | 0.92 | 0.049 | 0.05 |
| JH02 | Feb 2019 | 13 | 7.6 | 8.41 | 3.82 | 1.80 | 0.67 | 0.030 | 0.06 |
| JH03 | Mar 2019 | 20 | 16.5 | 8.85 | 37.67 | 1.21 | 1.16 | 0.086 | 0.05 |
| JH04 | Apr 2019 | 41 | 19.4 | 8.59 | 25.66 | 1.97 | 0.70 | 0.058 | 0.06 |
| JH05 | May 2019 | 15 | 25.2 | 9.19 | 12.01 | 1.44 | 0.84 | 0.082 | 0.15 |
| JH06 | Jun 2019 | 43 | 28.5 | 9.51 | 26.21 | 1.75 | 1.35 | 0.087 | 0.33 |
| JH07 | Jul 2019 | 27 | 34.3 | 8.93 | 42.04 | 0.77 | 0.68 | 0.031 | 0.10 |
| JH08 | Aug 2019 | 18 | 31.0 | 8.61 | 36.58 | 1.06 | 1.50 | 0.125 | 0.14 |
| JH09 | Sep 2019 | 17 | 25.9 | 8.49 | 22.93 | 1.04 | 1.06 | 0.078 | 0.31 |
| Lake Jinniu | | | | | | | | | |
| JN10 | Oct 2018 | 9 | 29.0 | 6.56 | 24.70 | 1.83 | 3.37 | 0.120 | 2.38 |
| JN11 | Nov 2018 | 15 | 26.0 | 6.60 | 40.18 | 0.51 | 8.73 | 1.000 | 1.67 |
| JN12 | Dec 2018 | 18 | 17.0 | 6.70 | 21.83 | 0.43 | 12.38 | 0.920 | 7.05 |
| JN01 | Jan 2019 | 17 | 20.0 | 6.20 | 115.40 | 8.06 | 11.61 | 0.300 | 5.65 |
| JN02 | Feb 2019 | 22 | 23.0 | 6.70 | 165.00 | 1.64 | 9.86 | 0.490 | 1.04 |
| JN03 | Mar 2019 | 38 | 25.0 | 6.70 | 45.80 | 4.47 | 4.96 | 0.180 | 1.77 |
| JN04 | Apr 2019 | 15 | 26.0 | 6.50 | 105.80 | 5.80 | 2.88 | 0.020 | 0.34 |
| JN05 | May 2019 | 38 | 26.0 | 6.50 | 215.90 | 5.34 | 3.46 | 0.180 | 0.26 |
| JN06 | Jun 2019 | 12 | 25.5 | 7.12 | 107.80 | 4.95 | 4.15 | 0.260 | 2.54 |
| JN07 | Jul 2019 | 9 | 25.5 | 6.70 | 36.48 | 5.07 | 6.73 | 0.090 | 1.51 |
| JN08 | Aug 2019 | 14 | 25.5 | 6.40 | 156.38 | 4.82 | 3.41 | 0.150 | 1.64 |
| JN09 | Sep 2019 | 28 | 25.0 | 6.40 | 74.63 | 6.05 | 4.02 | 0.190 | 1.18 |

Tem: water temperature, Chl-*a*: chlorophyll *a* content, DO: dissolved oxygen concentration.

## 3. Results

### *3.1. Temporal variation in environmental variables*

Throughout the sampling period, in Lake Yunlong, Lake Jinghu and Lake Jinniu, the highest water temperatures occurred in June 2019, July 2019, and October 2018, and the lowest water temperatures occurred in February 2019, November and December 2018, and December 2018, respectively (Table 1).

Preprints (www.preprints.org) | NOT PEER-REVIEWED | Posted: 14 December 2023 doi:10.20944/preprints202312.1103.v1



Among the three lakes, amplitude in fluctuation of pH was the greatest in Lake Yunlong, and the smallest in Lake Jiuniu; the opposites was true for TP and $NH_4^+$-N concentrations, and densities of cladocerans and copepods. Amplitudes in fluctuation of chl-a concentration and TN content was the greatest in Lake Jiuniu, and the smallest in Lake Jinghu; the opposites was true for density of the rotifer Asplanchna. Amplitude in fluctuation of dissolved oxygen concentration was the greatest in Lake Yunlong, and the smallest in Lake Jinghu (Table 1, Figure 1).

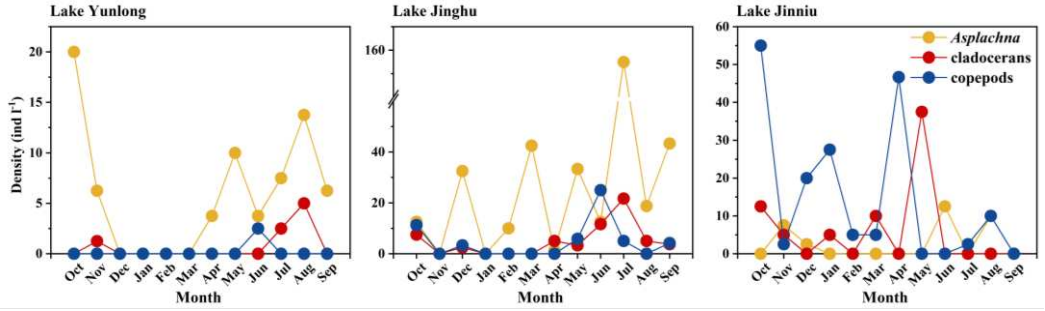


**Figure 1.** Temporal fluctuations of the densities of Asplanchna, cladocerans, and copepods in Lake Yunlong, Lake Jinghu and Lake Jinniu.

*3.2. Sequence variation, phylogenetic relationships, and COI/ITS1 group diagnosis*

A 632-bp fragment of mtCOI and a 270-bp fragment of nuITS1 were generated from 790 individuals within the *B. calyciflorus* species complex collected from the three lakes. All mtCOI and nuITS1 sequences have been deposited in GenBank (accession numbers ON114186-ON114975 and ON119425-ON120215, respectively). In 790 mtCOI sequences, a total of 316 polymorphic sites, including 217 parsimony informative sites, defined 44 unique haplotypes. In 790 nuITS1 sequences, a total of 62 polymorphic sites, with 46 parsimony informative sites, resulted in 22 unique haplotypes. Most haplotypes occurred in single samples in each lake at a given time, but a few haplotypes were shared by two or more samples from two or three lakes (Tables S1 & S2).

The Maximum-Likelihood phylogenetic tree reconstructed using the COI sequences showed that the *B. calyciflorus* species complex consisted of five distinct groups ("6", "11" and "13 - 15"; Figure 2), and that reconstructed using the ITS1 sequences showed that the *B. calyciflorus* species complex consisted of three distinct groups ("A", "C" and "D"; i.e. three species: *B. dorcas*, *B. calyciflorus* s.s., and *B. fernandoi*, respectively; Figure 2). Based on the mtCOI dataset, the GMYC model gave optimal solutions for two evolving entities. The estimate of 5 groups was provided by the ABGD model with 0.022 prior maximal distance, the estimated number of 10 groups was provided by the PTP method. Based on nuITS1 dataset, the GMYC model gave optimal solutions for 33 evolving entities. The estimate of 1 group was provided by the ABGD model with 0.022 prior maximal distance, and the estimate of 3 groups was provided by the PTP method. According to Papakostas et al. [43], we chose the more conservative number of entities. Hence, the five COI clades were identified as five COI groups, and named "6", "11", "13", "14", and "15", following Papakostas et al. [43]. The three ITS1 clades were also identified as three distinct groups ("A", "C", and "D"; i.e. three species: *B. dorcas*, *B. calyciflorus* s.s., and *B. fernandoi*, respectively). COI groups "6", "11", "13", "14", and "15" comprised 14, 43, 3, 1, and 34 COI haplotypes, and ITS1 groups "A" (*B. dorcas*), "C" (*B. calyciflorus* s.s.), and "D" (*B. fernandoi*) comprised 3, 45, and 9 ITS1 haplotypes, respectively (Figure 2).

Preprints (www.preprints.org) | NOT PEER-REVIEWED | Posted: 14 December 2023 doi:10.20944/preprints202312.1103.v1



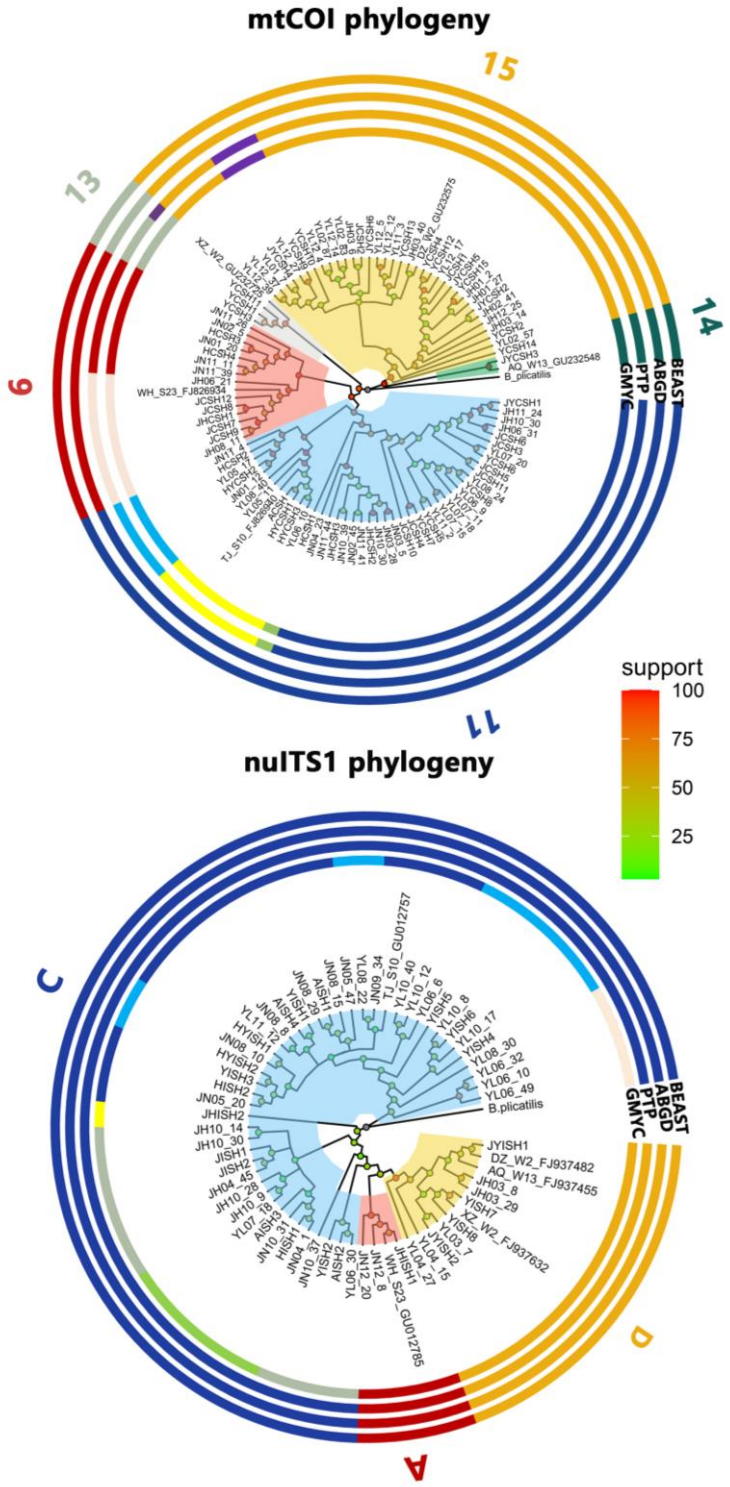


**Figure 2.** The Maximum-Likelihood phylogenetic trees and DNA taxonomy results of the Brachionus calyciflorus species complex based on the mtCOI and nuITS1 sequences from Lake Yunlong, Lake Jinghu and Lake Jinniu. "A", "C", and "D" represent *B. dorcas*, *B. calyciflorus* s.s., and *B. fernandoi*, respectively.

*3.3. Temporal distributions, relative frequencies, and densities of COI/ITS1 groups*

In Lake Yunlong, the *B. calyciflorus* species complex comprised four COI groups "11", "13", "14", and "15", or two ITS1 groups "C" (*B. calyciflorus* s.s.) and "D" (*B. fernandoi*). COI groups "11" and "15", or ITS1 groups "C" and "D", underwent clear seasonal successions. In October 2018, the *B. calyciflorus* species complex comprised exclusively COI group "11", or ITS1 group "C". In November

Preprints (www.preprints.org) | NOT PEER-REVIEWED | Posted: 14 December 2023 doi:10.20944/preprints202312.1103.v1



2018, COI groups "15" or ITS1 group "D" appeared and overlapped with "11" or "C". From December 2018 to April 2019, COI group "15" displaced "11" alone or with "14" and/or "13", and ITS1 group "D" replaced "C". During the overlapping periods of COI group "15" and other COI groups, or ITS1 groups "D" and "C", the relative frequency and density of COI group "15", or ITS1 group "D" was always higher. From May 2019 on, COI group "15", or ITS1 group "D" was displaced by "11" or "C" (Figures 3 and 4).

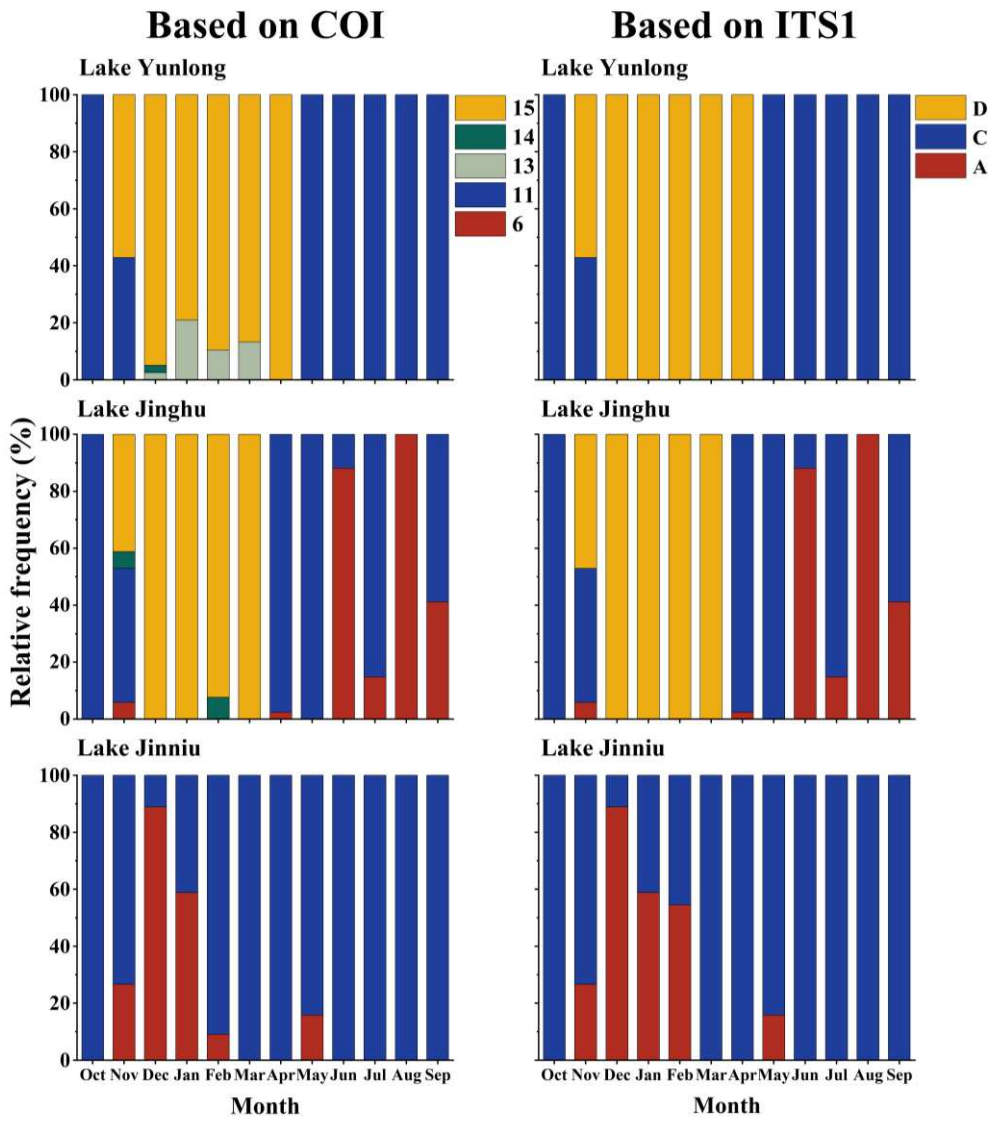


**Figure 3.** Relative frequencies of cryptic Brachionus calyciflorus groups in Lake Yunlong, Lake Jinghu and Lake Jinniu. "A", "C", and "D" represent *B. dorcas*, *B. calyciflorus* s.s., and *B. fernandoi*, respectively.

Preprints (www.preprints.org) | NOT PEER-REVIEWED | Posted: 14 December 2023 doi:10.20944/preprints202312.1103.v1



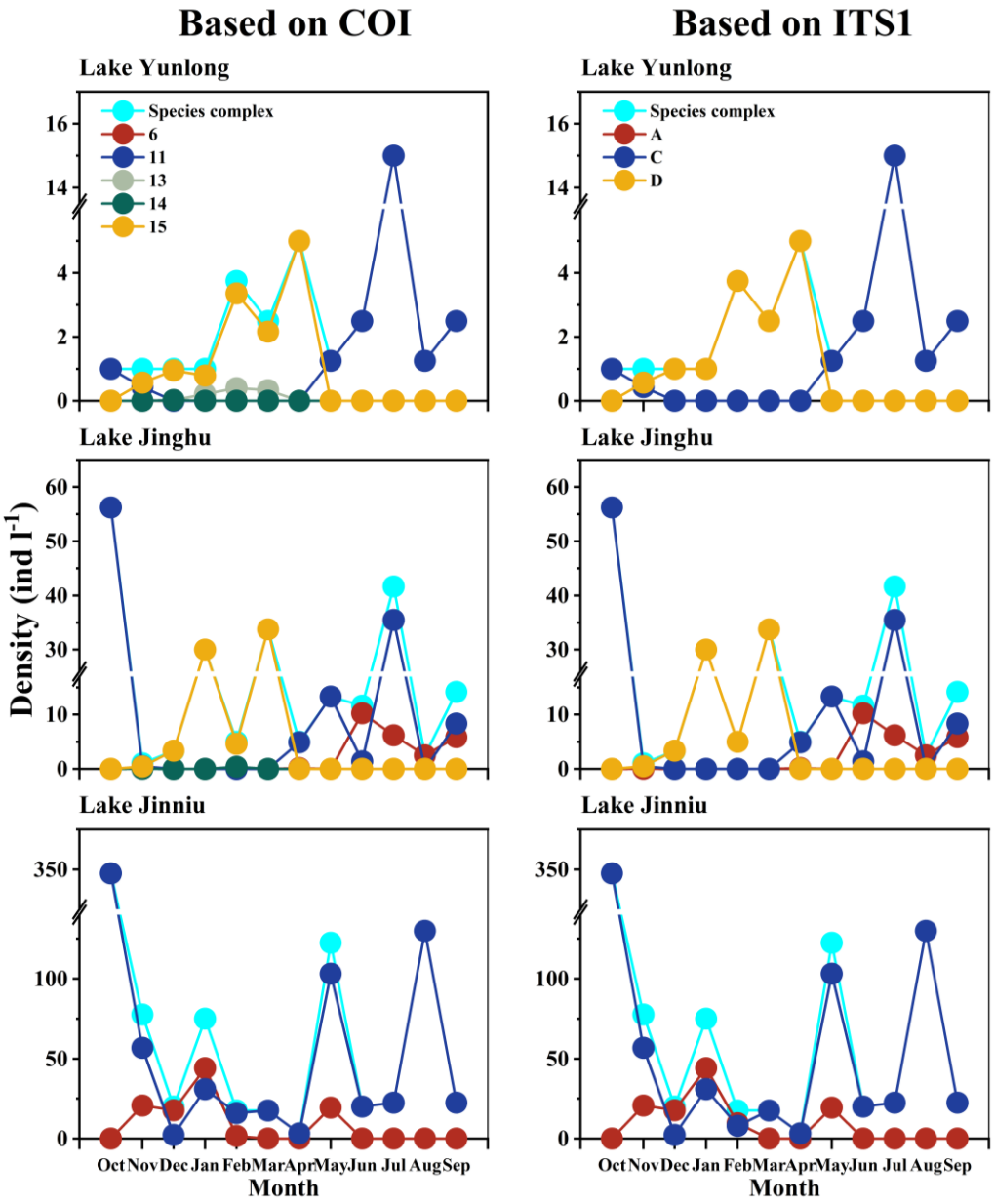


**Figure 4.** Densities of cryptic Brachionus calyciflorus groups and the *B. calyciflorus* species complex in Lake Yunlong, Lake Jinghu and Lake Jinniu. "A", "C", and "D" represent *B. dorcas*, *B. calyciflorus* s.s., and *B. fernandoi*, respectively. "S-C" represents the species complex.

In Lake Jinghu, the species complex comprised four COI groups "6", "11", "14", and "15", or three ITS1 groups "A" (*B. dorcas*), "C" (*B. calyciflorus* s.s.) and "D" (*B. fernandoi*). COI groups "15", and "11" and "6", or ITS1 groups "D", and "C" and "A" underwent clear seasonal successions. In October 2018, the species complex comprised exclusively COI group "11", or ITS1 group "C". In November 2018, COI groups "15", "14" and "6", or ITS1 groups "D" and "A" appeared and overlapped with "11" or "C". Between December 2018 and March 2019, COI group "15" displaced "11" alone or with "14", with "15" having a much higher relative frequency and density than "14"; ITS1 group "D" displaced "C". Between April and May 2019, COI group "11" or ITS1 group "C" displaced "15" or "D" alone or with "6"or "A", with "11" or "C" having a much higher relative frequency and density than "6" or "A". Between June and August 2019, COI group "6" or ITS1 group "A" overlapped with "11" or "C" and finally displaced "11" or "C". During the overlapping period of COI groups "6" and "11", or ITS1 groups "A" and "C", "11" or "C" had a lower relative frequency and density than "6" or "A" in June, and the opposite was true in July and September 2019 (Figures 3 and 4).

 doi:10.20944/preprints202312.1103.v1



In Lake Jinniu, the species complex comprised two COI groups "6" and "11", or two ITS1 groups "A" (*B. dorcas*) and "C" (*B. calyciflorus* s.s.). Throughout the sampling period, COI group "11" or ITS1 group "C" existed in the water body. Between November 2018 and February 2019, and in May 2019, COI group "6" or ITS1 "A" appeared and overlapped with "11" or "C". COI group "6" had a higher relative frequency and density than "11" between December 2018 and January 2019, and the opposite was true in the other months. Between December 2018 and February 2019, ITS1 group "A" had a higher relative frequency and density than "C", and the opposite was true in November 2018 and May 2019 (Figures 3 and 4).

*3.4. Effects of environmental variables on the relative frequencies and densities of COI/ITS1 groups*

Principal component analysis (PCA) of water environmental variables in Lake Yunlong and Lake Jinghu revealed two factors to explain 99.02% and 99.67% of the total variance, respectively. Water temperature was positively correlated with factor 1 ($F_1$, accounting for 41.45% and 63.84% of the data variance in Lake Yunlong and Lake Jinghu, respectively) and factor 2 ($F_2$, accounting for 90.75% and 76.55% of the data variance in Lake Yunlong and Lake Jinghu, respectively); chl-a concentration was correlated positively with factor 1 ($F_1$, accounting for 90.93% and 76.81% of the data variance in Lake Yunlong and Lake Jinghu, respectively), and negatively with factor 2 ($F_2$, accounting for 41.20% and 63.99% of the data variance in Lake Yunlong and Lake Jinghu, respectively). When the frequency of each group in each sample collected from these two lakes were represented in the space defined by $F_1$ and $F_2$ scores, respectively, there were straightforward discriminations among cold- and warm-water groups. COI groups "13", "14" and "15", and ITS1 group "D" (*B. fernandoi*) could be considered cold-water groups because they were associated with low $F_2$ values (low temperature), and COI groups "11" and "6", and ITS1 group "C" (*B. calyciflorus* s.s.) and "A" (*B. dorcas*) could be considered warm-water groups because they were associated with high $F_2$ values (high temperature) (Figure 5). The generalized linear model (GLM) analyses showed that in Lake Yunlong the densities of COI group "11" and ITS1 group "C" were significantly affected by water temperature and chl-a concentration (all $p < 0.01$), and those of COI group "15" and ITS1 group "D" were significantly affected by water temperature, chl-a concentration and their interaction (all $p < 0.01$). In Lake Jinghu, the densities of COI groups "6", "11" and "15", and ITS1 groups "A", "C" and "D" were significantly affected by water temperature, chl-a concentration and their interaction (all $p < 0.05$) (Table 2).

## 4. Discussion

This study found five mtCOI groups ("15", "14", "13", "11" and "6"), and three nuITS1groups ("A", "C", and "D"; i.e. three species: *B. dorcas*, *B. calyciflorus* s.s., and *B. fernandoi*, respectively) within the *B. calyciflorus* species complex in Yunlong, Jinghu and Jnniu lakes, which indicated a remarkably mito-nuclear discordance. Cryptic *B. calyciflorus* species (i.e. ITS1 groups) displayed different temporal distribution patterns among the three lakes. In Lake Yunlong, *B. fernandoi* and *B. calyciflorus* s.s. underwent a clear seasonal succession, which was largely attributed to their differential adaptation to water temperature. In Lake Jinghu, *B. fernandoi*, *B. calyciflorus* s.s. and *B. dorcas* exhibited both seasonal succession and temporal overlap. Seasonal successions were largely attributed to their differential adaptation to temperature, and temporal overlap resulted from their differential responses to algal food concentration. In Lake Jinniu, *B. calyciflorus* s.s. persisted throughout the year, and overlapped with *B. dorcas* for five months. Temporal overlap resulted from their differential responses to copepod predation.

Preprints (www.preprints.org) | NOT PEER-REVIEWED | Posted: 14 December 2023 doi:10.20944/preprints202312.1103.v1



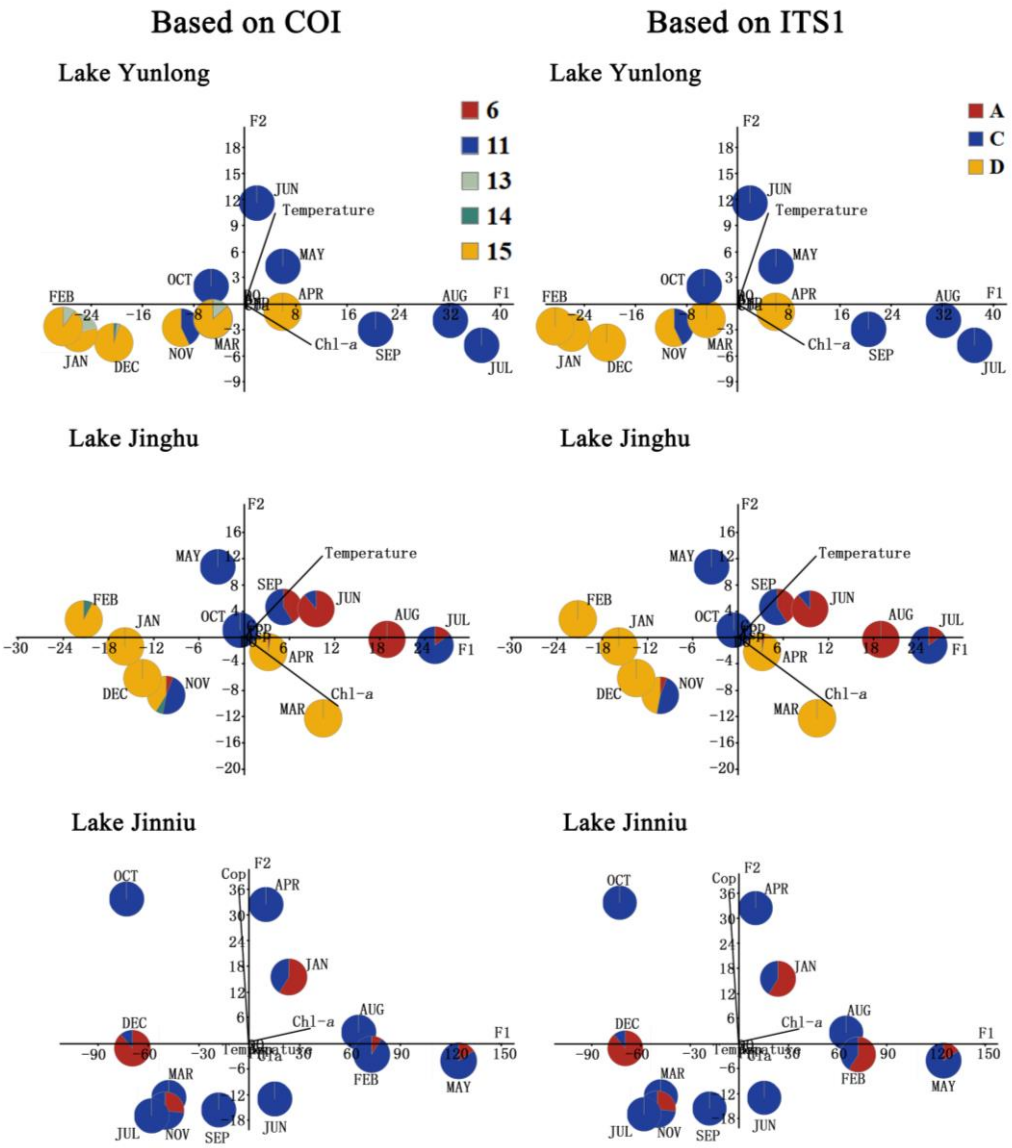


**Figure 5.** Principal component analyses on the environmental variables (temperature, pH, DO, chl-*a* concentration, and the densities of *Asplanchna*, copepods and cladocerans) in Lake Yunlong, Lake Jinghu and Lake Jinniu. Three variables (the densities of *Asplanchna*, copepods and cladocerans) in both Lake Yunlong and Lake Jinghu, and five variables (water temperature, TP and dissolved oxygen concentrations, and the densities of *Asplanchna* and cladocerans) in Lake Jinniu were very strongly skewed and were transformed to lg ($x$+1) or lg $x$ (only for water temperature). "DO" represents dissolved oxygen, "Asp." represents *Asplanchna*, "Cop." represents copepods, and "Cla." represents cladocerans.

Mito-nuclear discordance (i.e. discordance between mtDNA and nuclear phylogenies) across taxa is increasingly recognized as a major challenge to species delimitation based on DNA sequence data [53]. With respect to the *B. calyciflorus* complex, remarkably mito-nuclear discordances were observed between mitochondrial and nuclear groups, and species delimitation based on the ITS1 marker has proved to be more reliable predictors of morphological variation than delimitation using the mitochondrial COI gene [30,43,54]. In this study, we found 5 mtCOI groups and 3 nuITS1 groups within the *B. calyciflorus* species complex in the three lakes that had been sequenced for both the COI and ITS1 markers, which indicated a remarkably mito-nuclear discordance. Mito-nuclear discordance is often attributed to differences in levels of male and female ongoing gene flow [55], and suggests interspecific gene introgression and hybridization among lineages [56]. Hybridization amongst the

 doi:10.20944/preprints202312.1103.v1



species of the *B. calyciflorus* species complex has already been demonstrated [43] and further supported by crossing experiments [57]. Sympatric distribution of species promotes gene introgression/hybridization [58].

**Table 1.** Effects of principal environmental variables on densities of the main mtCOI/nuITS1 groups in Lake Yunlong, Lake Jinghu and Lake Jinniu using GLMs.

| Groups | | Lake Yunlong | | | Lake Jinghu | | | Lake Jingniu | | |
|---|---|---|---|---|---|---|---|---|---|---|
| | | Tem (A) | Chl-*a* (B) | A × B | Tem (A) | Chl-*a* (B) | A × B | Cop (A) | Chl-*a* (B) | A × B |
| "6" | *z* | - | - | - | 30.01 | 23.26 | -25.54 | -13.405 | 5.603 | 23.279 |
| | *P* | - | - | - | $<2\times10^{-16***}$ | $<2\times10^{-16***}$ | $<2\times10^{-16***}$ | $<2\times10^{-16***}$ | $<2.11\times10^{-8***}$ | $<2\times10^{-16***}$ |
| "11" | *z* | 8.978 | 4.923 | -0.916 | 36.892 | -1.924 | -4.899 | 273.1 | 140.3 | -171.5 |
| | *P* | $<2\times10^{-16***}$ | $8.53\times10^{-7***}$ | 0.36 | $<2\times10^{-16***}$ | 0.0544 | $9.65\times10^{-7***}$ | $<2\times10^{-16***}$ | $<2\times10^{-16***}$ | $<2\times10^{-16***}$ |
| "13" | *z* | -0.109 | -0.611 | -1.312 | - | - | - | - | - | - |
| | *P* | 0.913 | 0.541 | 0.19 | - | - | - | - | - | - |
| "15" | *z* | -4.526 | 12.448 | -13.961 | 85.53 | 55.86 | -74.39 | - | - | - |
| | *P* | $6.02\times10^{-6***}$ | $<2\times10^{-16***}$ | $<2\times10^{-16***}$ | $<2\times10^{-16***}$ | $<2\times10^{-16***}$ | $1.06\times10^{-9***}$ | - | - | - |
| "A" | *z* | - | - | - | 30.21 | 23.30 | -25.59 | -12.39 | 14.86 | 21.52 |
| | *P* | - | - | - | $<2\times10^{-16***}$ | $<2\times10^{-16***}$ | $<2\times10^{-16***}$ | $<2\times10^{-16***}$ | $<2\times10^{-16***}$ | $<2\times10^{-16***}$ |
| "C" | *z* | 8.978 | 4.923 | -0.916 | 36.576 | -2.045 | -4.667 | 273.4 | 139.4 | -171.1 |
| | *P* | $<2\times10^{-16***}$ | $8.53\times10^{-7***}$ | 0.36 | $<2\times10^{-16***}$ | $0.0408^{*}$ | $3.05\times10^{-6***}$ | $<2\times10^{-16***}$ | $<2\times10^{-16***}$ | $<2\times10^{-16***}$ |
| "D" | *z* | -4.98 | 11.81 | -13.41 | 74.21 | 51.74 | -66.63 | - | - | - |
| | *P* | $6.35\times10^{-7***}$ | $<2\times10^{-16***}$ | $<2\times10^{-16***}$ | $<2\times10^{-16***}$ | $<2\times10^{-16***}$ | $<2\times10^{-16***}$ | - | - | - |

Tem: water temperature, Chl-a: chlorophyll a content, Cop: Copepod density. A: *B. dorcas*, C: *B. calyciflorus* s.s., D: *B. fernandoi*. *** 0.001, ** 0.01, * 0.05.

Michaloudi et al. reviewed the geographical distribution of the *B. calyciflorus* species complex: *B. calyciflorus* s.s. has a cosmopolitan distribution, whereas *B. dorcas* occurs in Palearctic, Tropical, Oriental and Australian regions, and *B. elevatus* and *B. fernandoi* are distributed in Palearctic and Oriental regions [59]. Yang et al. found that *B. calyciflorus* s.s. occurs in the Eastern Plain and Yunnan-Guizhou Plateau in China, *B. dorcas* is restricted to the Eastern Plain, *B. elevatus* occurs in the Eastern Plain, Northeast Plain, Inner Mongolia-Xinjiang Plateau and Qinghai-Tibetan Plateau, and *B. fernandoi* is distributed in the Eastern Plain, Inner Mongolia-Xinjiang Plateau and Qinghai-Tibetan Plateau [54]. In this study, *B. calyciflorus* s.s. occurs in all three lakes, but the opposite was true for *B. elevates*. *B. dorcas* was not detected in the samples from Lake Yunlong, and *B. fernandoi* was not detected in those collected from Lake Jinniu. Considering the short life cycle and fast reproductive ability of these rotifer species, a higher frequency of sampling is necessary in future studies.

Zooplankters dwell in temporally variable habitats where large-scale changes in their abiotic and biotic environments may impact population demographic and genetic structure. Consequently, many zooplankton species occur during restricted seasons, and sympatric species can occur in seasonal succession [60]. For example, some cryptic *B. plicatilis* species in ponds and lakes undergo seasonal succession, although others overlap for short or long periods [8,14–18]. *B. fernandoi*, and *B. calyciforus* s.s. and *B. dorcas* within the *B. calyciflorus* species complex in Lake Tingtang also display seasonal succession [30]. In this study, *B. calyciflorus* s.s. and *B. fernandoi* in Lake Yunlong displayed seasonal succession; *B. fernandoi*, and *B. dorcas* and *B. calyciflorus* s.s. in Lake Jinghu displayed seasonal successions, although *B. dorcas* and *B. calyciflorus* s.s. overlap for a long period. *B. calyciflorus* s.s. and *B. dorcas* in Lake Jinniu did not exhibit seasonal succession. These results supported the hypothesis that the temporal distribution pattern of cryptic *B. calyciforus* species varies with different climate zones. It should be noted that following the framework provided by the theory of coexistence in

 doi:10.20944/preprints202312.1103.v1



fluctuating environments [61,62], the short-term disappearance of *B. dorcas* and *B. calyciforus* s.s. from the water column of Lake Jinghu (in May and August 2019, respectively) did not necessarily involve species exclusion.

Because of their short generation times and complex life cycles, the seasonal succession of zooplankton species often correlates with abiotic conditions, indicating certain levels of ecological specialization [7,13]. Seasonal succession of some cryptic *B. plicatilis* species in coastal Mediterranean ponds is largely explained by their differential adaptation to combinations of salinity and temperature [8,14–16,19–21], and such succession in an inland salt lake (Lake Koronia, Greece) is because of differential ecological preferences to water temperature [18]. Seasonal succession of *B. fernandoi*, and *B. calyciforus* s.s. and *B. dorcas* in Lake Tingtang is also explained by differences in their adaptation to water temperature [30–32]. Identical results were obtained in this study. *B. fernandoi* had a preference to lower water temperatures (3.2 °C - 18.9 °C in Lake Yunlong, and 5.6 °C - 16.5 °C in Lake Jinghu), but the opposite was true for *B. calyciforus* s.s. and *B. dorcas* (16.7 °C - 28.7 °C in Lake Yunlong, 19.4 °C - 34.3 °C in Lake Jinghu, and 17.0 °C - 29.0 °C in Lake Jinniu). We therefore considered *B. fernandoi* as a cold-water species, and *B. calyciforus* s.s. and *B. dorcas* as warm-water species, corresponding to heat-sensitive and heat-tolerant species, respectively [32].

How competing species coexist is a fundamental ecological question (Gabaldón et al., 2015). Two hypotheses have been advanced to explain the temporal overlap of cryptic *B. plicatilis* and *B. calyciflorus* species: i) that sufficient resources and the natural environmental fluctuations allow these species to coexist [8,29]; and ii) that the stable coexistence of potentially strongly competitive cryptic species may be a result of their differential responses to environmental conditions such as salinity [8,14–21] and oxygen availability [22], resource partitioning and differential vulnerability to predators [23–26,29,30]. This study showed that the synchronous coexistence of *B. calyciflorus* s. s. and *B. dorcas* in Lake Jinghu results from their differential responses to algal food concentration, and that in Lake Jinniu is because of their differential responses to copepod predation. These results supported the hypothesis that the mechanisms underlying the temporal overlap of potentially strong competitors are different between climate zones.

## 5. Conclusions

In Lake Yunlong, *B. fernandoi* and *B. calyciflorus* s.s. underwent a clear seasonal succession, which was largely attributed to their differential adaptation to water temperature. In Lake Jinghu, *B. fernandoi*, *B. calyciflorus* s.s. and *B. dorcas* exhibited both seasonal succession and temporal overlap. Seasonal successions were largely attributed to their differential adaptation to temperature, and temporal overlap resulted from their differential responses to algal food concentration. In Lake Jinniu, *B. calyciflorus* s.s. persisted throughout the year, and overlapped with *B. dorcas* for five months. Temporal overlap resulted from their differential responses to copepod predation. These results indicated that the temporal distribution pattern of cryptic *B. calyciforus* species and the mechanism allowing competitor coexistence vary with different climate zones. Further studies of additional lakes in each climatic zone are essential to know the generality of this conclusion.

**Supplementary Materials:** The following are available online at the website of this paper posted on Preprints.org., Table S1: Shared mtCOI haplotypes among all 790 individuals of *B. calyciflorus* complex. Table S2: Shared nuITS1 haplotypes among all 790 individuals of *B. calyciflorus* complex.

**Author Contributions:** Conceptualization, Y.X., Y.L.G and Y.L.X.; conducting the research, Y.X., L.L.G., Y.J.W. and H.F.; data analysis, Y.X., Y.L.X., X.F.C., X.L.X. X.L.W., and Y.L.G; preparation of figures and tables, Y.X., Y.L.G and Y.L.X.; data interpretation and writing: Y.X., Y.L.X., L.L.G., X.F.C., X.L.X., X.L.W., Y.J.W., H.F. and Y.L.G. All authors have read and agreed to the published version of the manuscript.

**Funding:** This work was supported by the Natural Science Foundation of China (grant nos. 31971562, 31470015) and University Synergy Innovation Program of Anhui Province (grant no. GXXT-2020- 075).

**Data Availability Statement:** Not applicable.

**Acknowledgments:** The authors are grateful to Dr. Shi-Niu Dai, Dr. Han Zhu, and Mr. Fan Gao for their assistance in figure preparation and data analyses.

**Conflicts of Interest:** The authors declare no conflict of interest.

## References


1. Knowlton, N. Sibling species in the sea. *Annu. Rev. Ecol. Evol. S.* **1993**, *24*, 189-216.
2. Schonrogge, K.; Barr, B.; Wardlaw, J.C.; Napper, E.; Gardner, M.G.; Breen, J.; Elmes, G.W.; Thomas, J.A. When rare species become endangered: cryptic speciation in myrmecophilous hoverflies. *Biol. J. Linn. Soc.* **2002**, *75*, 291-300.
3. Bickford, D.; Lohman, D.J.; Sodhi, N.S. Cryptic species as a window on diversity and conservation. *Trends Ecol. Evol.* **2007**, *22*, 148-155.
4. Dayrat, B. Towards integrative taxonomy. *Biol. J. Linn. Soc.* **2005**, *85*, 407-415.
5. Puillandre, N.; Lambert, A.; Brouillet, S.; Achaz, G. ABGD, automatic barcode gap discovery for primary species delimitation. *Mol. Ecol.* **2012**, *21*, 1864-1877.
6. Leibold, M.; McPeek, M. Coexistence of the niche and neutral perspectives in community ecology. *Ecology* **2006**, *87*, 1399-1410.
7. Gabaldón, C.; Fontaneto, D.; Carmona, M.J.; Montero-Pau, J.; Serra, M. Ecological differentiation in cryptic rotifer species: what we can learn from the *Brachionus plicatilis* complex. *Hydrobiologia* **2017**, *796*, 7-18.
8. Ortells, R.; Gómez, A.; Serra, M. Coexistence of cryptic rotifer species: ecological and genetic characterization of *Brachionus plicatilis*. *Freshwater Biol.* **2003**, *48*, 2194-2202.
9. Nicholls, B.; Racey, P.A. Contrasting home-range size and spatial partitioning in cryptic and sympatric pipistrelle bats. *Behav. Ecol. Sociobiol.* **2006**, *61*, 131–142.
10. Wellborn, G.A.; Cothran, R.D. *Niche diversity in crustacean cryptic species: complementarity in spatial distribution and predation risk*. Oecologia Springer, Berlin/Heidelberg, 2007; pp 154: 175–183.
11. Leibold, M.A. The niche concept revisited: mechanistic models and community context. *Ecology* **1995**, *76*, 1371–1382.
12. Chase, J.; Leibold, M. *Ecological Niches: linking Classical and Contemporary Approaches*. University of Chicago Press, Chicago, 2003.
13. Walczyńska A,; Fontaneto D.; Kordbacheh A.; Hamil S.; Jimenez-Santos M.A.; Paraskevopoulou S.; Pociecha A.; Zhang W. Niche differentiation in rotifer cryptic species complexes: a review of environmental effects. *Hydrobiologia* 2023. https://doi.org/10.1007/s10750-023-05291-7
14. Gómez, A.; Temprano, M.; Serra, M. Ecological genetics of a cyclical parthenogen in temporary habitats. *J. Evol. Biol.* **1995**, *8*, 601-622.
15. Gómez, A.; Carmona, M.J.; Serra, M. Ecological factors affecting gene flow in the *Brachionus plicatilis* complex (Rotifera). *Oecologia*, **1997**, *111*, 350-356.
16. Montero-Pau, J.; Ramos-Rodríguez, E.; Serra, M.; Gómez, A. Long-term coexistence of rotifer species. *PloS One* **2011**, *6*, 1-9.
17. Gabaldón, C.; Montero-Pau, J.; Serra, M.; Carmona, M.J. Morphological similarity and ecological overlap in two rotifer species. *PloS One* **2013**, *8*, e57087.
18. Papakostas, S.; Michaloudi, E.; Triantafyllidis, A.; Kappas, I.; Abatzopoulos, T.J. Allochronic divergence and clonal succession: two microevolutionary processes sculpturing population structure of *Brachionus* rotifers. *Hydrobiologia* **2013**, *700*, 33-45.
19. Campillo, S.; García-Roger, E.M.; Carmona, M.J.; Serra, M. Local adaptation in rotifer populations. *Evol. Ecol.* **2010**, *25*, 933-947.
20. Gabaldón, C.; Serra, M.; Carmona, M.J.; Montero-Pau, J. Life-history traits, abiotic environment and coexistence: the case of two cryptic rotifer species. *J. Exp. Mar. Biol. Ecol.* **2015**a, *465*, 142- 152.
21. Gabaldón, C.; Carmona, M.J.; Montero-Pau, J.; Serra, M. Long-term competitive dynamics of two cryptic rotifer species: diapause and fluctuating conditions. *PLoS One* **2015**b, *10*, e0124406.
22. Walczyńska, A.; Serra, M. Body size variability across habitats in the *Brachionus plicatilis* cryptic species complex. *Sci. Rep.-UK* **2022**, *12*, 6912.
23. Ciros-Pérez, J.; Carmona, M.J.; Serra, M. Resource competition between sympatric cryptic rotifer species. *Limnol. Oceanog.* **2001**, *46*, 1511-1523.
24. Ciros-Pérez, J.; Carmona, M.J.; Lapesa, S.; Serra, M. Predation as a factor mediating resource competition among rotifer cryptic species. *Limnol. Oceanog.* **2004**, *49*, 40-50.
25. Lapesa, S.; Snell, T.W.; Fields, D.M. Selective feeding of *Arctodiaptomus salinus* (Copepoda, Calanoida) on co-occurring cryptic rotifer species. *Freshwater Biol.* 2004, *49*, 1053-1061.
26. Li, L.; Niu, C.J.; Ma, R. Rapid temporal succession identified by COI of the rotifer *Brachionus calyciflorus* Pallas in Xihai Pond, Beijing, China, in relation to ecological traits. *J. Plankton Res.* **2010**, *32*, 951-959.
27. Li, Y.; Xi, Y.-L.; Wang, A.; Niu, X.; Wen, X.; Liu, G. Temporal variation in composition of *Brachionus calyciflorus* complex and life history traits of sibling species in Lake Tingtang. *Acta Ecol. Sin.* **2014**, *34*, 6172-

6181.
28. Niu, X.; Xi, Y.-L.; Li, Y.; Wang, A.; Liu, G. Rapid change in structure of *Brachionus calyciflorus* complex collected from Jiulian Pond and its ecological mechanism. *J. Appl. Ecol.* **2013**, *24*, 3561- 3566.
29. Wen, X.-L.; Xi, Y.-L.; Zhang, G.; Xue, Y.-H.; Xiang, X.-L. Coexistence of cryptic *Brachionus calyciflorus* (Rotifera) species: roles of environmental variables. *J. Plankton Res.* **2016**, *38*, 478- 489.
30. Zhang, Y.; Zhou, A.; Xi, Y.-L.; Sun, Q.; Ning, L.-F.; Xie, P.; Wen X.-L.; Xiang, X.-L. Temporal patterns and processes of genetic differentiation of the *Brachionus calyciflorus* (Rotifera) complex in a subtropical shallow lake. *Hydrobiologia* 2018, *807*, 313-331.
31. Zhang, W.; Lemmen, K.D.; Zhou, L.; Papakostas, S.; Declerck, S.A. Patterns of differentiation in the life history and demography of four recently described species of the *Brachionus calyciflorus* cryptic species complex. *Freshwater Biol*. **2019**, *64*, 1994-2005.
32. Paraskevopoulou, S.; Dennis, A.B.; Weithoff, G.; Tiedemann, R. Temperature-dependent life history and transcriptomic responses in heat-tolerant versus heat-sensitive *Brachionus* rotifers. *Sci. Rep.-UK* **2020**, *10*, 13281.
33. Wen, X.-L.; Xi, Y.-L.; Qian, F.P.; Zhang, G.; Xiang, X.-L. Comparative analysis of rotifer community structure in five subtropical shallow lakes in east China: role of physical and chemical conditions. *Hydrobiologia* **2011**, *661*, 303-316.
34. Huang, X.-F. *Survey, Observation and Analysis of Lake Ecology*. Chinese Standard Press, Beijing, 1999.
35. Montero-Pau, J.; Gómez, Á; Muñoz, J. Application of an inexpensive and high-throughput genomic DNA extraction method for the molecular ecology of zooplanktonic diapausing eggs. *Limnol. Oceanog.* **2008**, *6*, 218-222.
36. Folmer, O.; Black, M.; Hoeh, W. DNA primers for amplification of mitochondrial cytochrome coxidase subunit I from diverse metazoan invertebrates. *Mol. Mar. Biol. Biotechnol.* **1994**, *3*, 294- 299.
37. Xi, Y.-L.; Chen, Y.-Q.; Zhuge, Y.; Huang, X.-F. Sequence analysis of rDNA 18S-28S intergenic spacer regions from *Brachionus calyciflorus*, *B. bidentata*, *B. diversicornis* and *B. angularis* in lake Donghu, China. *Acta Hydrobiol. Sin.* **2003**, *27*, 427-430.
38. Sara, H. Bioinformatik: BLAST. *Biologie in unserer Zeit* **2018**, *48*, 367-368.
39. Posada, D.; Crandall, K.A. Modeltest: testing the model of DNA substitution. *Bioinformatics* **1998**, *9*, 817-818.
40. Ronquist, F.; Huelsenbeck, J.P. MRBAYES 3: Bayesian Phylogenetic inference under mixed models. *Bioinformatics 2003*, **19**, 1572-1574.
41. Xiang, X.-L.; Xi, Y.-L.; Wen, X.-L.; Zhang, G.; Wang, J.-X.; Hu, K. Patterns and processes in the genetic differentiation of the *Brachionus calyciflorus* complex, a passively dispersing freshwater zooplankton. *Molecular Phylogenet. Evol.* **2011**a, *59*, 386-398
42. Xiang, X.-L.; Xi, Y.-L.; Wen, X.-L.; Zhang, G.; Wang, J.-X.; Hu, K. Genetic differentiation and phylogeographical structure of the *Brachionus calyciflorus* complex in eastern China. *Mol. Ecol.* **2011**b, *20*, 3027-3044.
43. Papakostas, S.E.; Michaloudi, K.; Proios, M.; Brehm, L.; Verhage, J.; Rota, J.; Peña, C.; Stamou, G.; Pritchard, V.L.; Fontaneto, D.; Declerck, S.A.J. Integrative taxonomy recognizes evolutionary units despite widespread mitonuclear discordance: evidence from a rotifer cryptic species complex. *Syst. Biol.* **2016**, *65*, 508-24.
44. Fontaneto, D.; Kaya, M.; Herniou, E.A.; Barraclough, T.G. Extreme levels of hidden diversity in microscopic animals (Rotifera) revealed by DNA taxonomy. *Mol. Phylogenet. Evol.* **2009**, *53*, 182- 189.
45. Mills, S.; Alcántara-Rodríguez, J.A.; Ciros-Pérez, J.; Gómez, A.; Hagiwara, A.; Galindo, K.H.; Walsh, E.J. Fifteen species in one: deciphering the *Brachionus plicatilis* species complex (Rotifera, Monogononta) through DNA taxonomy. *Hydrobiologia* **2017**, *796*, 39-58.
46. Puillandre, N.; Modica, M.V.; Zhang, Y.; Sirovich, L.; Boisselier, M.C.; Cruaud, C.; Holford, M.; Samadi, S. Large-scale species delimitation method for hyperdiverse groups. *Mol. Ecol*. **2012**, *21*, 2671-2691.
47. Zhang, J.-J.; Kapli, P.; Pavlidis, P.; Stamatakis, A. A general species delimitation method with applications to phylogenetic placements. *Bioinformatics* **2013**, *29*, 2869-2876.
48. Fontaneto, D.; Iakovenko, N.; Eyres, I.; Kaya, M.; Wyman, M.; Barraclough, T.G. Cryptic diversity in the genus *Adineta* Hudson & Gosse, 1886 (Rotifera: Bdelloidea: Adinetidae): a DNA taxonomy approach. *Hydrobiology* **2011**, *662*, 27-33.
49. Fontaneto, D.; Flot, J.F.; Tang, C.Q. Guidelines for DNA taxonomy with a focus on the meiofauna. *Marine Biodivers.* **2015**, *45*, 433-451.
50. Sanderson, M.J. Estimating absolute rates of molecular evolution and divergence times: a penalized likelihood approach. *Mol. Biol. Evol.* **2002**, *19*, 101-109.
51. Xi, Y.-L.; Li, H.-B.; Cheng, X.-F. Morphometric differences among three cryptic species in *Brachionus*

*calyciflorus* species complex. *Acta Ecol. Sin.* **2010**, *30*, 3645-3653.
52. R Core Team. R: A language and environment for statistical computing version 4.2.2. R Foundation for Statistical Computing, Vienna, Austria, 2022. URL: https://www.R-project.org/.
53. Schlick-Steiner, B.C.; Arthofer, W.; Steiner, F.M. Take up the challenge! Opportunities for evolution research from resolving conflict in integrative taxonomy. *Mol. Ecol*. **2014**, *23*, 4192- 4194.
54. Yang, W.; Deng, Z.; Blair, D.; Hu; W.; Yin, M. Phylogeography of the freshwater rotifer *Brachionus calyciflorus* species complex in China. *Hydrobiologia* **2022**, *849*, 2813-2829.
55. Avise, J.C., *Phylogeography: the History and Formation of Species*. Harvard University Press, Massachusetts, **2000**.
56. Petit, R.; Excoffier, L. Gene flow and species delimitation. T*rends Ecol. Evol*. **2009**, *24*, 386-393.
57. Zhang, W., Declerck, S.A.J. Intrinsic postzygotic barriers constrain cross-fertilisation between two hybridising sibling rotifer species of the *Brachionus calyciflorus* species complex. *Freshwater Biol*. **2022**, *67*, 240-249.
58. Hebert, P. Interspecific hybridization between cyclic parthenogens. *Evolution* **1985**, *39*, 216-220.
59. Michaloudi, E,; Papakostas, S.; Stamou, G.; Nedela, V.; Tihlarikova, E.; Zhang, W.; Declerck, S. Reverse taxonomy applied to the *Brachionus calyciflorus* cryptic species complex: Morphometric analysis confirms species delimitations revealed by molecular phylogenetic analysis and allows the (re)description of four species. *PLoS One* **2018**, *13*, e0203168.
60. King, C.E.; Serra, M. Seasonal variation as a determinant of population structure in rotifers reproducing by cyclical parthenogenesis. *Hydrobiologia* **1998**, *387/388*, 361-372.
61. Chesson, P. Mechanisms of maintenance of species diversity. *Annu. Rev. Ecol. Evol. S.* **2000**, *31*, 343- 366.
62. Chesson, P.; Huntly, N. The roles of harsh and fluctuating conditions in the dynamics of ecological communities. *Am. Nat*. **1997**, *150*, 519-553.